INT. J. REMOTE SENSING, 1993, VOL. 14, NO. 14, 2665–2676

A united model for quantitative remote sensing of suspended sediment concentration

LI XIA

Guangzhou Institute of Geography, Guangzhou 510070,
People's Republic of China

(Received 17 February 1992; in final form 11 September 1992)

Abstract. A remote sensing technique has been developed for quickly detecting suspended sediment concentration and monitoring the transport and deposition of suspended sediment in a large estuary area. There is an agreement that the best wave band to analyse suspended sediment concentration is 0·6–0·8 μm (MSS 5 and TM 3 for Landsat), but it is suggested that there is a divergence between which model is used to study the suspended sediment best. This paper presents a unified model for a quantitative approach to suspended sediment concentration using remote sensing. The comparison between various models with field investigation data and published data has shown that the unified model has a higher correlation and precision than most popular models used currently. The author illustrates that the logarithm model is flawed when suspended sediment concentration is high. The unified model has been applied to the quantitative remote sensing of suspended sediment in Lingdingyang, the Pearl River estuary (the biggest river in South China). Further improvement to the unified model with TM3/TM5 ratio technique has also been proposed to minimize the background influences (atmospheric and solar effects). Results show that the improved unified model has more advantages than other models which usually need a large number of field data each time they are used. The improved united model can be applied to a global scale after its parameters are classified according to different regions.

1. Introduction

Confined by operation conditions, conventional investigation involves hard field work to locate many sites for the accurate mapping of the distribution of suspended sediment in a large water area. Since satellite remote sensing has a great advantage in a quantitative approach of suspended sediment concentration, many efforts have been made in the study of relevant wave bands and models. There is an undoubted conclusion that the 0·6–0·8 μm wave band is best sensitive to suspended sediment concentration and remote sensing data in the wave band (MSS 5 and TM 3 bands for Landsat) are of very high correlativity with the concentration. As the radiation transfer processes in water are very complicated, many models have been proposed to obtain the relation between remote sensing data and suspended sediment concentration. The linear relevant relation was the earliest model used to estimate suspended sediment concentration from remote sensing data. Klemas *et al.* (1974) proposed the logarithm relevant relation when he applied remote sensing method to study Delaware Bay. Munday and Alföldi (1979) proved that the logarithm relation is better than the linear relation for remote sensing of suspended sediment concentration. Philpot (1981) presented the radiative transfer model for remote sensing of vertically inhomogeneous water. In China, remote sensing research on suspended sediment have been carried out in Bohai Bay, the Yellow River estuary, the Yangtze estuary and the Pearl River estuary. We initiated the study in the Pearl River estuary in 1985 (Gu *et al.* 1990). Li Jing (1986) proposed a negative index model in his study in East China.

Those models are:

1.1. *The Linear model*

$$R = A + BS \tag{1}$$

Where R is the reflectance, S is the suspended sediment concentration and A and B are relevant coefficients.

This is the earliest model proposed to simulate the relation between suspended sediment concentration and remote sensing data. However, because it is of its limited form and its tendency to be highly erroneous, its use is usually limited in the early stage of remote sensing application.

1.2. *The Logarithm model*

$$R = A + B \log S \tag{2}$$

This formula can only depict the relation between suspended sediment concentration and remote sensing data well when the concentration is not too high within a small range of concentration distribution. It should be noted that great discordance may appear in high concentrations when the distribution range is large, since it is applied extensively.

1.3. *The Gordon model*

$$R = C + S/(A + B\,S)$$

or

$$1/(R - C) = B + A/S \tag{3}$$

Where A, B and C are parameters. This is based on a quasi-single-scattering radiative approximative model (Gordon 1973) that is used less popularly than the logarithm formula.

1.4. *The Negative index model*

$$R = A + B(1 - e^{-DS})$$

or

$$\ln (D - L) = A + B\,S \tag{4}$$

Where A, B and D are parameters and L is brightness. The negative index model developed by Li Jing (1986) makes some improvement for high concentration, but discrepancy still exists because of adopting some approximative condition.

Since there has not been any satisfactory model of high precision and practical status until now, this paper proposes a unified model to overcome the discrepancy in high concentrations and an improved unified model with ratio technique to minimize the environmental background influences for global scale application purposes.

2. The unified model for quantitative remote sensing of suspended sediment concentration

Suppose that downward radiation in the sea water is $E_d(Z,\lambda)$ which decreases as water depth Z increases and that the attenuation coefficient is $K(Z,\lambda)$ which consists of two parts, water absorption coefficient $\alpha(Z,\lambda)$ and backscattering coefficient $\beta(Z,\lambda)$. Radiation diffuses after it enters water so that

$$\frac{\partial E_d(Z,\lambda)}{\partial Z} = -K(Z,\lambda)E_d(Z,\lambda)$$

and

$$E_d(Z,\lambda) = E_d(0,\lambda)\exp\left\{-\int_0^Z K(h,\lambda)dh\right\} \tag{5}$$

The upwelling radiation $E_u(0,\lambda)$ above the water surface comes from back scattering. Suppose that the penetrative depth of remote sensing is h_0 which varies little when suspended sediment concentration is over $10\,\mathrm{g\,l^{-1}}$ based on the research by Whitlock (1976).

We have

$$\begin{aligned}
E_u(0,\lambda) &= E_d(0,\lambda)\int_0^{h_0}\beta(h,\lambda)\exp\left[-2\int_0^h K(\xi,\lambda)d\xi\right]dh \\
&\doteq E_d(0,\lambda)\int_0^{h_0}\beta(h,\lambda)\exp\left[-2\bar{K}(\lambda)h\right]dh \\
&\doteq -E_d(0,\lambda)\frac{\bar{\beta}(\lambda)}{2\bar{K}(\lambda)}\left[\exp\left[-2\bar{K}(\lambda)h\right]\right]_0^{h_0} \\
&= E_d(0,\lambda)\frac{\bar{\beta}(\lambda)}{2\bar{K}(\lambda)}\{1-\exp\left[-2\bar{K}(\lambda)h_0\right]\}
\end{aligned} \tag{6}$$

$$\begin{aligned}
\text{Reflectance } R &= \frac{E_u(0,\lambda)}{E_d(0,\lambda)} \\
&= \frac{\bar{\beta}(\lambda)}{2\bar{K}(\lambda)}\{1-\exp\left[-2\bar{K}(\lambda)h_0\right]\}
\end{aligned} \tag{7}$$

Here $\bar{\beta}(\lambda)$ and $\bar{K}(\lambda)$ are mean value of $\beta(h,\lambda)$ and $K(h,\lambda)$ in vertical h direction. Water scattering is due to the scattering of water molecule and scattering of suspended sediment (Cracknell 1981).

$$\bar{\beta}(\lambda) = a + bS \tag{8}$$

Where a is the scattering of water molecule, and b is the scattering coefficient of suspended sediment. Water absorption is due to the absorption of water molecule and absorption of suspended sediment.

$$\bar{\alpha}(\lambda) = a' + b'S \tag{9}$$

Where $\acute{a}$ is the absorption of water molecule, and b' is the absorption coefficient of suspended sediment.

Then

$$\bar{K}(\lambda)=\bar{\alpha}(\lambda)+\bar{\beta}(\lambda) \tag{10}$$

$$\begin{aligned} R &= \frac{a+bS}{2(a+a')+2(b+b')S}\{1-e^{-2[(a+a')+(b+b')S]h_0}\} \\ &= \frac{a+bS}{a''+b''S}(1-e^{-a''h_0-b''h_0S}) \\ &= (C+S/(A+BS))(1-ke^{-b''h_0S}) \\ &= (C+S/(A+BS))(1-ke^{-DS}) \\ &= \text{Gordon}(S)\text{Index}(S) \end{aligned} \tag{11}$$

The model includes the Gordon equation and the negative index equation. The linear equation and the logarithm equation can also be deduced by the approximation of the model.

1. When the penetrative depth h is indefinitely deep, that is

$$h_0 \rightarrow \infty$$

or

$$e^{-DS} \rightarrow 0$$

Then Index(S)→constant

$$R=\text{Gordon}(S) \tag{12}$$

2. When the absorption and scattering of water molecules can be ignored, the

$$a=0 \text{ and } a'=0$$

or

$$\frac{a+bS}{a''+b''S} \rightarrow \text{constant}$$

Then

$$\text{Gordon}(S) \rightarrow \text{constant}$$

$$R=\text{Index}(S) \tag{13}$$

3. When e^{-DS} of Index(S) is expanded by the series and approximate terms are selected, we can have the terms equivalent to the linear model and the logarithm model (Li Jing 1986).

There is a relation between radiative brightness L received by the detector of remote sensing and ground reflectance R

$$L=L_p+\frac{E_{ad}}{\pi}RT \tag{14}$$

Where L_p is the path-radiated brightness of the atmosphere, T is the transmissivity of the atmosphere and E_{ad} is the downward radiation on the water surface. They can be considered as constant in the same remote sensing image. If we replace R in formula (11) by L, then

$$L=A+B(S/(G+S))+C(S/(G+S))e^{-DS} \tag{15}$$

Table 1. Brightness value L of MSS-5 (31 August 1978; Guangzhou, P. R. China; flood season) and quasi-simultaneous suspended sediment concentration S in the Pearl River estuary.

Brightness L	55	70	83	54	46	58	72	78
Content S ($mg\,l^{-1}$)	50	120	430	54	29	60	175	248

A, B and C are relevant coefficients and G, D are parameters to be determined in regression. $S/(G+S)$ term and $(S/(G+S))e^{-DS}$ term are relevant with remote sensing brightness L. G and D values are selected to achieve the highest relevant coefficient for the unified model by regression calculation. The practical procedure is: first fix D and select G to get the highest relevant coefficient; then fix G and select D to get the highest relevant coefficient. Repeating the procedure, the computer can find a group of proper G and D values very quickly. Results indicate that the correlation and precision of the unified model are higher than those of popular models used currently.

3. The comparison between various models and the application of the unified model in the Pearl River estuary

The conventional field data collected in the Pearl River estuary are applied to make a comparison between the different models. Published data in journal are also used to verify the models fairly.

These comparisons and results are set out in tables 1–8 as follows:

The results above indicate that the linear model shows the poorest correlation between remote sensing data and suspended sediment concentration and the least precision. The unified model is very satisfactory since the correlation coefficient is usually greatest (except in table 8 where the Gordon model has a slightly higher correlation coefficient than the unified model) and the error is the least. It is very important to know that the logarithm model is not a good model, because of the existence of a large error in the high suspended sediment concentration S of distribution in a wide range (usually when suspended sediment concentration $>300\,mg\,l^{-1}$). Since there are major shortcomings in the linear model, the logarithm

Table 2. Calculation results of each models.

Model \ Result	Formula	r	Error $\Delta L/\bar{L}$ (%)
Linear	$L=51{\cdot}9526+0{\cdot}0861S$	0·992	9·44
Logarithm	$L=-0{\cdot}3663+32{\cdot}3885\log S$	0·992	2·71
Gordon	$\frac{1}{L-26}=0{\cdot}0152+1{\cdot}0090/S$	0·996	2·32
Index	$\ln(84{\cdot}5-L)=3{\cdot}8052-0{\cdot}0079S$	0·996	2·98
Unified	$L=22{\cdot}2848+696{\cdot}5389S/(S+52)-631{\cdot}1757S/(S+52)\,e^{-0{\cdot}000008S}$	0·996	2·03

Table 3. Brightness value L of TM3 (10 December 1988; Guangzhou, P. R. China; dry season) and simultaneous suspended sediment concentration S in the Pearl River estuary.

Brightness L	36·6	39·7	40·9	33·9	36·5	43·6	33·5	36·6
Content S ($mg\,l^{-1}$)	82	90	92	38	66	95	48	87

model has still been very popularly used by many authors (Klemas *et al.* 1974, Curran 1987, Tassan 1988, Doerffer 1989, etc.). The negative index model and the Gordon model are fine, but not as good as the unified model. The form of the unified model

$$L = \text{Gordon}(S)\ \text{Index}(S)$$

has indicated that the Gordon model and the negative index model are an approximation to the unified model and that the linear model and the logarithm model are further approximations to the negative index model.

Meantime, the research also reveals that different sources of data can also result in the variation of correlation and error besides the form of models due to the error brought about by data sampling. A series of errors will be produced because of time differences between sampling and remote sensing, and the space differences between sample site and remote sensing pixel.

The remote sensing of suspended sediment technique has been carried out in the Pearl River estuary since 1985. Part of primary work was to determine suspended sediment concentration with MSS-5. Because the weather is usually cloudy in the Parl River area it is a difficult job to predict whenever the satellite can receive an ideal image and make a plan to sample simultaneous suspended sediment data for the image. Quasi- simultaneous data is usually used based on the periodicity of tide, run-off and wind, and some investigation data from the hydrological station in the Pearl River is also selected (see table 1).

The simple logarithm model was applied for relevant calculation in the primary study

Table 4. Calculation results of each model.

Model \ Result	Formula	r	Error $\Delta L/\bar{L}$ (%)
Linear	$L = 27{\cdot}4528 + 0{\cdot}1366S$	0·845	5·32
Logarithm	$L = 2{\cdot}2739 + 19{\cdot}0901 \log S$	0·810	5·83
Gordon	$\frac{1}{L-30} = -0{\cdot}0193 + 12{\cdot}0463/S$	0·890	5·66
Index	$\ln(100-L) = 4{\cdot}3663 - 0{\cdot}0031S$	0·835	5·79
Unified	$L = 52{\cdot}866 + 734{\cdot}6031S/(S+100) - 833{\cdot}5584S/(S+100)\,e^{0{\cdot}001S}$	0·901	3·89

Table 5. Reflectance R and suspended sediment concentration S in simulated condition (Shou Shourong and Chen Jian 1988).

Reflectance R	12·54	16·74	21·69	27·96	29·10	32·45	35·56	37·26	37·41	39·01	39·70	40·72	42·09	43·03	43·12
Content S ($mg\,l^{-1}$)	9·2	12·8	25·2	57·8	80·1	101·3	141·4	163·2	133·3	241·4	296·3	350·0	406·4	454·8	510·6

$$L = -0{\cdot}3663 + 32{\cdot}3885 \log S \tag{16}$$

where the correlation coefficient $r = 0{\cdot}992$ and mean relative error $= 2{\cdot}71$ per cent.

When the unified model was used the result was

$$L = 22{\cdot}2848 + 696{\cdot}5389S/(S+52) - 631{\cdot}1757(S/(S+52))\, e^{-0{\cdot}0000008S} \tag{17}$$

where the correlation coefficient $r = 0{\cdot}996$ and the mean relative error $= 2{\cdot}03$ per cent.

TM3 (10 December 1988, Guangzhou, P. R. China) and simultaneous investigation data were also obtained for relevant analysis. (See table 3.)

The result of the logarithm model was

$$L = 2{\cdot}2739 + 19{\cdot}0901 \log S \tag{18}$$

where the correlation coefficient $r = 0{\cdot}810$ and the mean relative error $= 5{\cdot}83$ per cent

The result of the unified model was

$$L = 52{\cdot}8660 + 734{\cdot}6031S/(S+100) - 833{\cdot}5584(S/(S+100))\, e^{-0{\cdot}001S} \tag{19}$$

where the correlation coefficient $r = 0{\cdot}901$, and the mean relative error $= 3{\cdot}89$ per cent.

The distribution of suspended sediment in the Pearl River estuary was calculated according to the united model, and an isoline map was produced after the slicing of concentration S into 8 classes (table 9 and figure 1).

The transport and deposition features of suspended sediment in the Pearl River estuary are revealed by the analysis of multi-phase Landsat images (25 December 1973, 24 December 1975, 10 February 1977, 31 August 1978, 1 October 1979, 7 February 1984, 30 July 1986, 8 December 1987, 10 December 1988, 13 October 1990). The suspended sediment concentratiopn is over $40\,mg\,l^{-1}$ (up to $400\,mg\,l^{-1}$)

Table 6. Calculation results of each model.

Model \ Result	Formula	r	Error $\Delta R/\bar{R}$ (%)
Linear	$R = 23{\cdot}5118 + 0{\cdot}0488S$	0·842	16·36
Logarithm	$R = -2{\cdot}8093 + 17{\cdot}4333 \log S$	0·992	3·76
Gordon	$\frac{1}{R-2} = 0{\cdot}0248 + 0{\cdot}6209/S$	0·993	7·30
Index	$\ln(43{\cdot}8 - R) = 3{\cdot}2350 - 0{\cdot}0070S$	0·983	7·26
Unified	$R = 7{\cdot}6448 + 85{\cdot}4495S/(S+45) - 49{\cdot}2464S/(S+45)\, e^{-0{\cdot}0001S}$	0·995	3·27

Table 7. Transformed brightness value L of NOAA-7 (4 November 1984; Hangzhou Bay) and simultaneous suspended sediment concentrations S (Li Jing 1986).

Brightness L	0·4789	0·4398	0·4398	0·3978	0·3978	0·2432	0·1985
Content S ($\mathrm{mg\,l^{-1}}$)	624·0	153·7	177·3	139·0	61·3	18·0	11·5

in the west part and below $20\,\mathrm{mg\,l^{-1}}$ in the east part of Lingdingyang in flood season; over $10\text{–}20\,\mathrm{mg\,l^{-1}}$ (up to $100\,\mathrm{mg\,l^{-1}}$) in the west part and below $5\,\mathrm{mg\,l^{-1}}$ in the east part in the dry season. Suspended sediment assembles largely in the shoals on the west part of Lingdingyang in the Pearl River estuary. The development of the shoals in this part is very fast because of sediment deposition and land reclamation. Based on the multitemporal image analysis, we consider that the life of the Pearl River estuary is 177–200 years and the estuary will be silted up within the period.

4. The further improvement of the unified model to minimize atmospheric influence

Many empirical models built from one group of conventional data could create a large error when they are applied in a different situation, such as in a new location or period. It is very inconvenient to obtain new data to revise the parameters of those models each time when they are used, especially in the cloudy area where simultaneous data are hard to collect for an idea image. Atmospheric correction is necessary to produce a more stable model which can be applied in a large region and over a long period. Among those radiation correction methods, the ratio technique has the obvious effect of reducing the atmospheric and solar influences. Since TM3 (or MSS5) is a most important band in the measurement of suspended sediment concentration, we need another new band in the unified model for the ratio correction, TM5 band is selected because it can indicate the atmospheric and solar background and make the correction calculation simple.

Because the downward radiation $E_d(Z, \lambda_5)$ of TM5 almost disappears when it enters the water, the upward radiation $E_u(0, \lambda_5)$ above the water could be considered to from back scattering on the water surface.

$$\begin{aligned} E_u(0, \lambda_5) &= E_d(0, \lambda_5)\beta(0, \lambda_5) \\ &= E_d(0, \lambda_5)b_5 S \end{aligned} \tag{20}$$

Table 8. Calculation results of each models.

Model \ Result	Formula	r	Error $\Delta L/\bar{L}$ (%)
Linear	$L=0{\cdot}3131+0{\cdot}0003S$	0·675	23·33
Logarithm	$L=0{\cdot}0453+0{\cdot}1691\log S$	0·956	9·22
Gordon	$\dfrac{1}{L-0{\cdot}06}=2{\cdot}3021+56{\cdot}3263/S$	0·997	4·27
Index	$\ln(0{\cdot}479-L)=-1{\cdot}1688-0{\cdot}0129S$	0·994	5·83
Unified	$L=0{\cdot}3683+0{\cdot}1596S/(S+270)-14{\cdot}9764S/(S+270)\,e^{-0{\cdot}1080S}$	0·994	3·99

Table 9. Concentration classes of suspended sediment in Lingdingyang of the Pearl River estuary.

Classes	I	II	III	IV	V	VI	VII	VIII
Content S ($\mathrm{mg\,l^{-1}}$)	$\leqslant 30$	31–50	51–100	101–150	151–200	201–300	301–400	$\geqslant 401$

where λ_5 is the wave band corresponding to TM5 and b_5 is the scattering coefficient of suspended sediment in TM5. The scattering of water molecules is small and is considered to be zero.

$$R_5 = \frac{E_u(0, \lambda_5)}{E_d(0, \lambda_5)} = b_5 S \tag{21}$$

where R_s is the reflectance in TM5 wave band.

When the scattering of water molecule is considered as 0, equation (11) can be expressed as

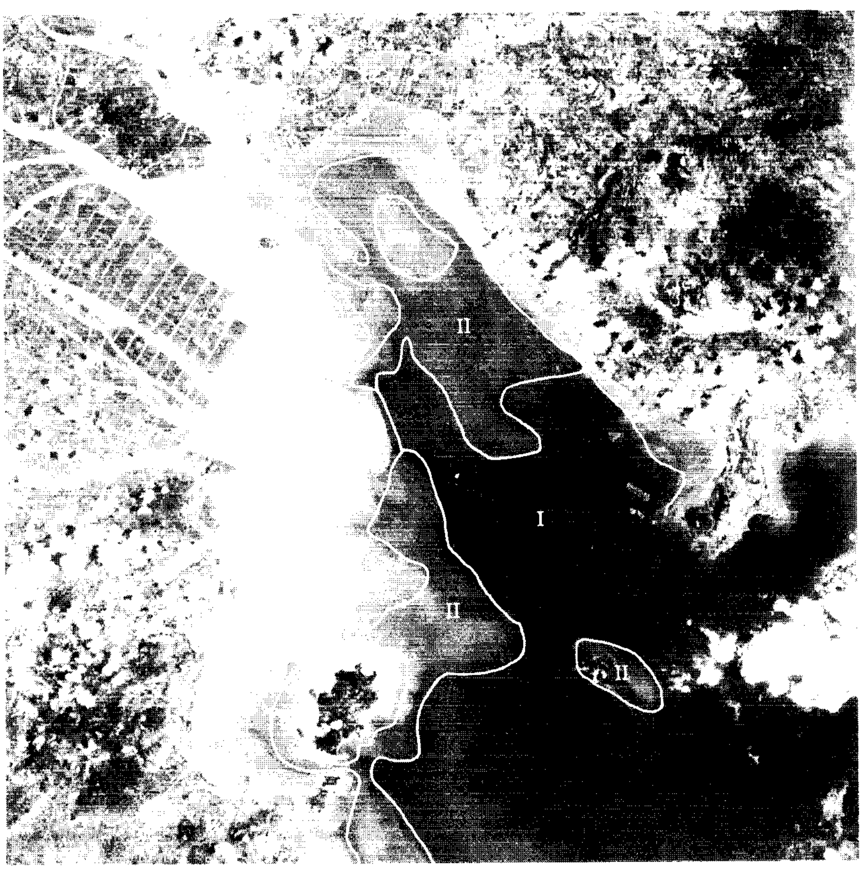

Figure 1. Classification of suspended sediment concentration in Lingdingyang of the Pearl River estuary (based on TM3, 3 July 1988).

$$R_3 = \frac{bS}{a'' + b''S}(1 - ke^{-DS}) \tag{22}$$

We have

$$\frac{R_3}{R_5} = \frac{b'''}{a'' + b''S}(1 - ke^{-DS}) \tag{23}$$

where a'', b'', and b''' are parameters.

Equation (10) can be expressed for the TM3 and TM5 bands as

$$TM3 = L_{p3} + \frac{E_{ad3}}{\pi} R_3 T_3 \tag{24}$$

$$TM5 = L_{p5} + \frac{E_{ad5}}{\pi} R_5 T_5 \tag{25}$$

Where L_{p3} and L_{p5} are path-radiated brightnesses of the atmosphere in the TM3 and TM5 wave bands; T_3 and T_5 are transmissivities of the atmosphere in the TM3 and TM5 wave bands; E_{ad3} and E_{ad5} are downward radiations of the TM3 and TM5 wave bands on the water surface. By the ratio of (24) and (25) we have

$$\frac{TM3 - L_{p3}}{TM5 - L_{p5}} = K\frac{R_3}{R_5} \tag{26}$$

Finally, there is

$$\frac{TM3'}{TM5'} = K\frac{R_3}{R_5} = \frac{A}{G+S} + \frac{B}{G+S}e^{-DS} + C \tag{27}$$

Because of the ratio features, the parameters A, B, C, D and G are relatively stable and the improved united model is more reliable than other popular used models when they are applied in various situations.

The improved united model was also verified by the Landsat TM3 (10 December 1988; Guangzhou, P. R. China) with conventional investigation data. The result was

$$TM'3/TM'5 = 430{\cdot}0950 - 500562{\cdot}8750/(130+S) + (446099{\cdot}4375/(130+S))\,e^{-0{\cdot}001S} \tag{28}$$

where correlation coefficient $r = 0{\cdot}920$ and the mean relative error $= 3{\cdot}42$ per cent.

Although there may be more than one group of parameters A, B, C, D and G suitable for each calculation, they are equivalent when they produce the same

Table 10. The predicted concentration S by various models.

Sample S ($\mathrm{mg\,l^{-1}}$)	Predicted concentration S ($\mathrm{mg\,l^{-1}}$): Logarithm error		Gordon error		Index error		Unified error		Improved unified error	
96	63	34%	70	27%	70	27%	77	20%	87	9%
73	47	35%	47	36%	58	21%	63	14%	66	10%
105	166	58%	138	31%	120	14%	108	3%	103	2%
129	209	62%	151	17%	138	7%	110	15%	132	2%

relevant coefficient and error. The significance of the improved unified model is its validity at another place and time after it has been set up, but other models are limited for use at sites where a large number of at least 'quasi-simultaneous' field data are available. The improved unified model and others set up with TM3 (10 December 1988; Guangzhou, P. R. China) and simultaneous field data in the Pearl River estuary are compared in their application to a different period, 3 July 1988, in the same area, in order to see which model is most high precise in a different situation.

The calculation above has indicated that the unified model and the improved unified model have less error than others. The improved unified model has the potential to become a global model after further study on sediment spectral characteristic of various regions have been made to obtain the different groups of parameters for each special region.

5. Conclusion

1. The paper presents a unified model of quantitative remote sensing of suspended sediment concentration

$$\begin{aligned} L &= \text{Gordon}(S)\ \text{Index}(S) \\ &= A + BS/(G+S) + C(S/(G+S))\, e^{-DS} \end{aligned}$$

which consists of the Gordon model and the negative index model. The linear model and the logarithm model are its further approximative forms.

2. The linear model is the poorest in application while the unified model is very satisfactory. Because the logarithm model which is extensively used, may create large errors its application should be limited.

3. The unified model succeeds in verification by conventional field data and published data, and in the application of quantitative remote sensing of suspended sediment concentration in Lingdingyang of the Pearl River estuary.

4. A practical model, the improved unified model is presented to minimize background influences (atmospheric and solar) with TM3/TM5 ratio

$$TM'3/TM'5 = A + B/(G+S) + C\, e^{-DS}/(G+S)$$

Results show that it is of a higher prediction precision than other popular models when they are applied to a different situation.

Acknowledgment

I would like to thank Mr Liu Oifang for his help in completing the paper.

References

CRACKNELL, A. P., 1981, Remote sensing in Meteorology. In *Oceanography and Hydrology* (Chichester: Ellis Horwood).

CURRAN, P. J., HANSON, J. D., PLUMMER, S. E., and PEDLEY, M. I., 1987, Multispectral remote sensing of nearshore suspended sediments: a pilot study. *International Journal of Remote Sensing*, **8,** 103–112.

DOERFFER, R., FISCHER, J., STOSSEL, M., and BROCKMANN, C., 1989, Analysis of thematic mapper data for studying the suspended matter distribution in the coastal area of the German Bight (North Sea). *Remote Sensing of Environment*, **28,** 61–73.

GORDON, H. R., and BROWN, O. B., 1973, Irradiance reflectivity of a flat ocean as a function of its optical properties. *Applied Optics*, **12,** 1549–1551.

GU QIUSHEN, RAO KAIYAN and LI XIA, 1990, *Remote sensing application in Lingdingyang estuary* (P. R. China: Science Press).

KLEMAS, V., BARTLETT, D., and PHILPOT, W., 1974, Coastal and estuarine studies with ERTS-1 and Skylab. *Remote Sensing of Environment*, **3,** 153–174.

LI JING, 1986, A study on determination of concentration of suspended sediment in water by remote sensing, *Acta Scientiae Circumstantiae*, **6,** 166–173.

MUNDAY, J. C., and ALFÖLDI, T. T., 1979, Landsat test of diffuse reflectance models for aquatic suspended solids measurement. *Remote Sensing of Environment*, **8,** 169–189.

PHILPOT, W., 1981, A radiative transfer model for remote sensing of inhomogeneous water. Ph.D. Dissertation, University of Delaware.

SHOU SHOURONG and CHEN JIAN, 1988, *Measurement and application of reflectance of remote sensing* (P. R. China: Science Press).

TASSAN, S., 1988, The effect of dissolved 'yellow substance' on the quantitative retrieval of chlorophyll and total suspended sediment concentrations from remote measurements of water colour. *International Journal of Remote Sensing*, **9,** 787–797.

WHITLOCK, C. H., 1976, An estimate of the influence of sediment concentration and type for various coastal waters. NASA NASA-TMX-73906.

WHITLOCK, C. H., WITTE, W. G. T. A., MORRIS, W. D., USRY, J. W., and POOLE, L. R., 1981, Research for reliable quantification of water sediment concentration from multispectral scanner remote sensing data. AGRISTARS report, CD-Z1-040788(JSC 17134), USDA/NASA.